Ultrasonics Sonochemistry 72 (2021) 105426

Contents lists available at ScienceDirect

Ultrasonics Sonochemistry

journal homepage: www.elsevier.com/locate/ultson

Conversion of silica by-product into zeolites by thermo-sonochemical treatment

Danutė Vaičiukynienė [a,*], Leonas Jakevičius [b], Aras Kantautas [a], Vitoldas Vaitkevičius [a], Vilimantas Vaičiukynas [d], Karel Dvořák [c]

[a] Kaunas University of Technology, Faculty of Civil Engineering and Architecture, Studentų g. 48, Kaunas 44249, Lithuania
[b] Kaunas University of Technology, Faculty of Mathematics and Natural Sciences, Studentų g. 52, Kaunas 44249, Lithuania
[c] Vytautas Magnus University, Faculty of Water and Land Management Agriculture Academy, Universiteto g. 10, Akademija 53361, Lithuania
[d] Brno University of Technology, Faculty of Civil Engineering, Veveří 512/95, Brno 602 00, Czechia

ARTICLE INFO

Keywords:
Silica by-product
Thermo-sonochemical treatment
Na-P zeolite
Na-X zeolite

ABSTRACT

The fine powdered silica by-product of processing of aluminum fluoride (fertilizer plant, Lithuania) was used for zeolite synthesis as silica and aluminum source. The effect of sonication time and the time of hydrothermal synthesis on crystallinity of the synthesized zeolite were studied. This allowed the transformation of the by-product to the mixture of Na–P zeolite and Na–X zeolite. It was determined that ultrasonic-assisted hydrothermal action effected the "diamond" shape formation of Na–P zeolite with clear crystal edges. Na–P zeolite had the morphology of pseudo-spherical forms constituted by small plates when hydrothermal treatment (without sonication) was use for the preparation of zeolites. Moreover, it was determined that ultrasonic-assisted hydrothermal method effected a reduction in the crystal size compared with the zeolites which were synthesized only by using hydrothermal synthesis. The total amount of zeolites as high as 88–93% was achieved after 24 h of hydrothermal treatment followed or unfollowed by sonication. By using longer duration (20 min) of ultrasound pretreatment it is possible to reduce the duration of hydrothermal synthesis: from 24 h to 12 h of hydrothermal treatment. In this case, similar results of total amount of zeolites were detected. In the present work, low-cost raw materials, such as silica by-product have been investigated for the production of zeolites.

1. Introduction

Generally, zeolites are synthesized from reagent materials by using hydrothermal synthesis as the main zeolite synthesis method. However many types of industrial waste based on aluminosilicates could be suitable as the initial materials for zeolite synthesis. By reusing production waste or using natural mineral materials instead of reagent raw materials it is possible to reduce the price of zeolite synthesis. Yoldi et al. [1] analyzed the main methods of zeolite synthesis using aluminosilicate-based by-products. Na–X, Na–Y, Na–A, Na–P and phillipsite were synthesized from some types of ashes: coal fly ash, biomass ashes, palm oil mill fly ash and bagasse fly ash. It was concluded that industrial wastes based on aluminosilicate compounds are suitable initial materials for the preparation of zeolites. Authors stated that the main properties and application fields of such type zeolites are like commercial zeolites made from reagent materials. Osacký et al. [2] used perlite by-product for the preparation of zeolite. The volcanic glass from perlite by-product converted to Phillipsite, zeolite P and zeolite X. The highest amount of zeolitic product reached 77 wt%. In the work [3] Na–X zeolite was synthesized from low aluminum coal fly ash. It was used hydrothermal method with fusion. The relative crystallinity of Na–X zeolite was controlled by time and temperature. The optimal temperature of synthesis was 90 °C and duration was 120 min. It was concluded that additional amount of aluminum had positive effect on the amount of Na–X zeolite in the synthesized products.

It was reported that the main methods of zeolite synthesis are conventional hydrothermal action, fusion, ultrasonic or microwave treatments [4–6]. Very often the combination of above-mentioned methods was used as well. Liu et al. [7] stated that Zeolite P was synthesized from Class C fly ash, as material rich in aluminum and silicon compounds, by using hydrothermal treatment. At temperatures under 120 °C the mixture of Na–P zeolite and quartz consisted the synthesis products. According to Abukhadra et al. [8] it is possible to synthesize the composite based on bentonite and zeolite-P by using bentonite as

* Corresponding author.
E-mail address: danute.vaiciukyniene@ktu.lt (D. Vaičiukynienė).

https://doi.org/10.1016/j.ultsonch.2020.105426
Received 5 August 2020; Received in revised form 8 December 2020; Accepted 9 December 2020
Available online 24 December 2020

Table 1
Chemical composition of the silica by-product, according XRF, wt%

Oxides	SiO_2	F	Al_2O_3	P_2O_5	CaO	Cl	Fe_2O_3	WO_3	Loss on ignition
	78.21	8.01	4.78	0.46	0.15	0.09	0.66	0.015	7.63

aluminosilicate material. The conventional hydrothermal treatment was used at 150 °C temperature for 4 h durations. In the study [9] Na–P - zeolite was received from coal fly ash. In this case hydrothermal method with ultrasound treatment was applied for the production of Na–P zeolite. The crystallinity of Na–P zeolite reached 87% when the duration of hydrothermal treatment was 1 h at 100 °C and the duration of sonication was 3 h. By using only sonochemical method Pal et al. [10] chemical reagents transformed to nano crystals of Na–P zeolite. The duration was 3 h and reactions were performed at room temperature. For zeolite crystallinity, the enlargement of irradiation energy and time had insignificant effect. In the study [11] waste glass and aluminum scraps were transformed to Na-FAU and Na–P1 zeolites. Hydrothermal treatment at 60 °C using with alkaline fusion was used. The crystallinity level of NaP1 phase varied from 42% to 80%.

In our previous work [12] it was determined that the zeolite NaA was synthesized from by-product silica by using ultrasound treatment at room temperature. In this case it reached the highest (25.81%) zeolite crystallinity and the synthesis were performed with suspensions aged for 24 h. Silica by-product is obtained from fertilizer plant (Lithuania). The utilization in cement systems of this silica by-product is problematic due the fluoride compounds in its composition. These fluoride compounds retarded the setting process and decreased the mechanical properties of hardened cement pastes or concretes as well. It was suggested thermal treatment [13] or chemical purification method of silica by-product [12,14]. All these suggestions are related with the elimination or neutralization of problematic fluoride compounds. Different situation is for zeolitic material synthesis. Kim et al. [15] stated that the pH of initial materials suspensions was much lower and the faster synthesis of zeolite in the systems with fluoride compounds was detected. In this case fluoride compound from silica by-product could act as mineralizing media.

In this work traditional hydrothermal treatment together with sonication was applied to synthesized Na–P zeolite from silica by-product. The higher crystallinity level of zeolites was received in comparison to our previous work [12].

2. Experimental

2.1. Experimental techniques

Chemical composition of silica by-product was determined according to the X-ray fluorescence (XRF). It was performed on an XRF spectrometer "Bruker X-ray S8 Tiger WD". Used Rh tube, anode voltage Ua up to 60 kV, current I to 130 mA.

A laser particle size analyzer "CILAS 1090 LD" determined the particle size distribution and the specific surface area of the materials in intervals from 0.04 to 500 μm. Loss on ignition was calculated after heating silica by-product at the temperature of 1000 °C.

Mineral composition of silica by-product and the products of synthesis such as gibbsite, Na-P zeolite and Na-X zeolite were evaluated aby using X-ray diffraction (XRD). The XRD analysis was performed on the "D8 Advance" diffractometer (Bruker AXS, Karlsruhe, Germany) operating at the tube voltage of 40 kV and tube current of 40 mA. The X-ray beam was filtered with a Ni 0.02 mm filter to select the CuKα wavelength. The powder X-ray diffraction patterns were identified with references available in the PDF-2 database. Quantification phase analyses of synthesis products were performed by the Rietveld method using the fundamental parameters approach [16].

The amount amorphous of phase was estimated using the "constant background intensity" method, in which the crystallinity of a sample is defined as the intensity ratio of the diffraction peaks and of the sum of all measured intensity - it can be calculated using an Eq. (1):

$$C = \frac{100 \cdot \sum I}{\sum I_{tot} - \sum I_{const.bgr.}} \quad (1)$$

where C is crystallinity in %, I is area of the crystalline peaks, I_{tot} is total area and $I_{const.bgr.}$ is area of the constant background. This constant background intensity is subtracted from the total intensity [20]. By separating all the crystalline peaks, the intensity of background was determined. The "Panalytical Highscore+ 3" program was used for the evaluation of amorphous phase.

The pH measurements of the water after washing were conducted by pH-meter EDGE, 230 V. NaF in water was defined with the HI-729 Fluoride Low Range Handheld Colorimeter, Checker®HC with a measuring range from 0 to 2.00 ppm (mg/L), a resolution of 0.01 ppm and an accuracy of ±0.05 ppm ±5% of reading.

Fourier transform infrared spectroscopy (FT-IR) were recorded with Perkin "Elmer FT-IR System" spectrometer. 1 mg of the substance was mixed with 200 mg of KBr and compressed in a forming press under vacuum for the IR analysis.

The microstructures of silica by-product and zeolitic products were investigated by using scanning electron microscopy (SEM) investigation method. A high-resolution scanning electron microscope "FEI Quanta 200 FEG" with a Schottky field emission gun (FEG) was used for this

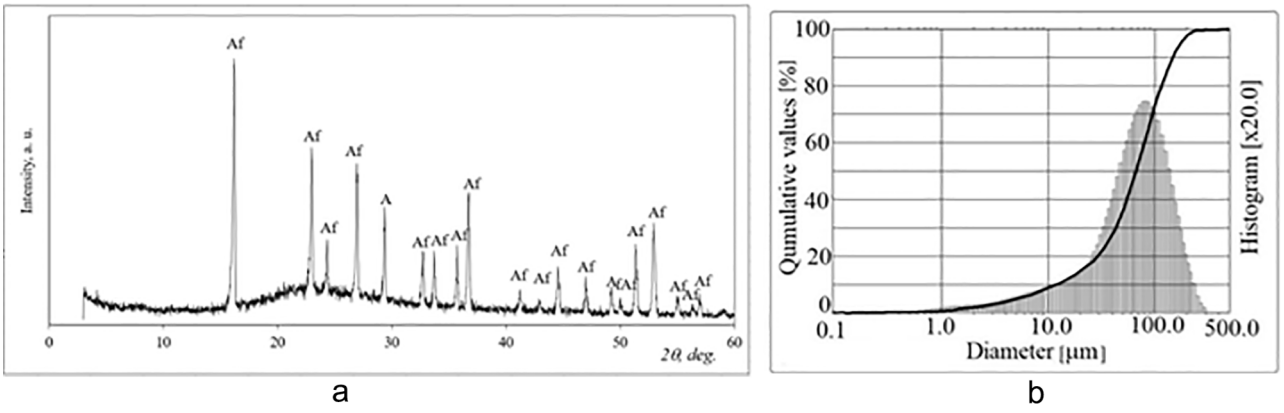

Fig. 1. The X-ray diffraction pattern (a) and particle size distributions (b) of silica by-product. Note: Af is aluminium fluoride hydrate $AlF_3 \cdot 3.5H_2O$ (35–827).

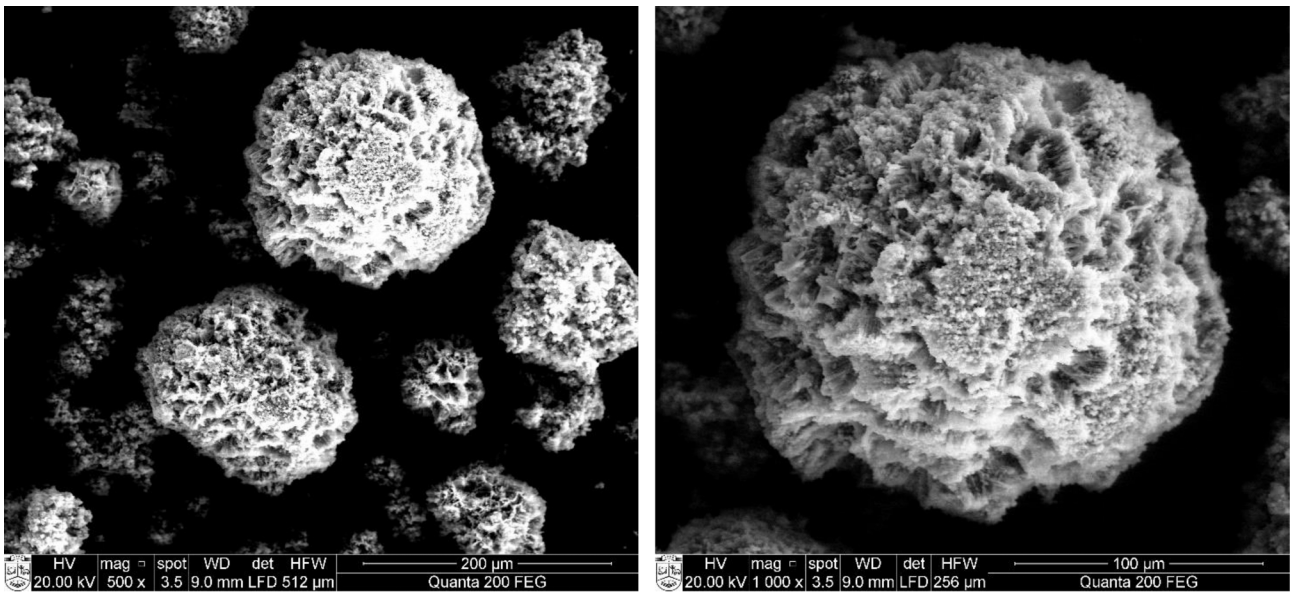

Fig. 2. The SEM images of silica by-product with different enlargement (a) and (b).

Table 2
The molar ratios of initial materials and the parameters of zeolite synthesis.

Samples	Molar ratio Na_2O:Al_2O_3:SiO_2:H_2O	Sonication time, min	Hydrothermal treatment time, h	The total amount of zeolites, %
0S3H	2:0.1:1:100	0	3	0
0S6H	2:0.1:1:100	0	6	0
0S12H	2:0.1:1:100	0	12	41.6
0S24H	2:0.1:1:100	0	24	92.8
5S3H	2:0.1:1:100	5	3	0
5S6H	2:0.1:1:100	5	6	0
5S12H	2:0.1:1:100	5	12	54.9
5S24H	2:0.1:1:100	5	24	87.8
10S3H	2:0.1:1:100	10	3	0
10S6H	2:0.1:1:100	10	6	1.6
10S12H	2:0.1:1:100	10	12	60.8
10S24H	2:0.1:1:100	10	24	92.2
20S3H	2:0.1:1:100	20	3	0
20S6H	2:0.1:1:100	20	6	9.1
20S12H	2:0.1:1:100	20	12	81.7
20S24H	2:0.1:1:100	20	24	91.3

purpose.

The conversion of silica by-product into zeolites by sonochemical method ultrasonic dispergation device BANDELIN electronic "UW3400" was used. Ultrasonication procedure lasted from 5 to 20 min using 20 kHz and 200 W power ultrasonic waves. Hydrothermal treatment was conducted in the kiln "SNOL 200/200".

2.2. Initial materials

Silica by-product is material based on amorphous SiO_2 polluted with fluoride compounds. This by-product was obtained from fertilizer plant (Lithuania) and it accumulated about 15,000 tons yearly [14]. Silica by-product is a silica hexaflouride acid neutralization product. Until now, the silica by-product has not been reused due to contaminated fluorine compounds and has accumulated in landfills. The are some works related with the neutralization of fluoride compounds from silica by-product by using $Ca(OH)_2$ and water suspension [17]. Kaminskas et al. [18] used silica by-product with clay and limestone to produce artificial pozzolana. In our previous works the negative effect of fluoride compounds was eliminated by thermally activating this silica gel [13]. In this work silica by-product was used as silica and aluminum sources.

According to oxide composition SiO_2 dominate in this silica by-product and it consist about 78 wt% (Table 1). There are about 8.01 wt% of fluoride and 4.78 wt% of aluminum oxide. The amount of other oxides does not exceed 1 wt%.

According to XRD analysis aluminium fluoride hydrate (as crystalline compound) dominate in silica by-product. In addition to this crystalline compound amorphous part can be identified. Fig. 1, a showed the amorphous hump in the rage of 17–35 (2θ).

The particle size distributions of silica by-product were shown in Fig. 1, b. The mean diameter of particles is 74.7 µm and specific surface area is about 716 m^2/kg.

The microstructure of silica by-product was investigated by using SEM analyze. It consisted irregular shape particles (Fig. 2 a). These particles have a large number of pores (Fig. 2 b).

Initial materials composition was shown in Table 2. The molar Na_2O:Al_2O_3:SiO_2:H_2O ratio was equal 2:0.1:1:100 for the zeolite synthesis [19]. A commercial reagents NaOH pellets (99% purity - DeltaChem, Czech Republic) and the additional amount of aluminum $Al(OH)_3$ (Lachema, Czech Republic) were used.

The mixture of silica by-product and aluminum hydroxide was mixed with the required amount of sodium hydroxide solution to a homogeneous state. In the first step, sonication treatment was conducted. The duration of this treatment was 0 min, 5 min, 10 min and 20 min (Table 2). In the second step, it was used hydrothermal method. The durations were 3 h, 6 h, 12 and 24 h at 95 °C temperature. After that solid part from liquid part was separated by using filtration. The excess of NaOH and NaF which form during alkali reaction were removed by washing with water. The excess of NaOH in washing water was evaluated with the measurement of pH. NaF in water was determined by using colorimetric method. Finally, powders were dried at dryer (24 h, 95 °C).

3. Results and discussion

3.1. The mineral composition of zeolitic products according XRD

The obtained powders of synthesis were characterized by XRD analysis. Fig. 1 shows the XRD patterns of synthesis products. The first series of zeolite synthesis was carried out by the conventional

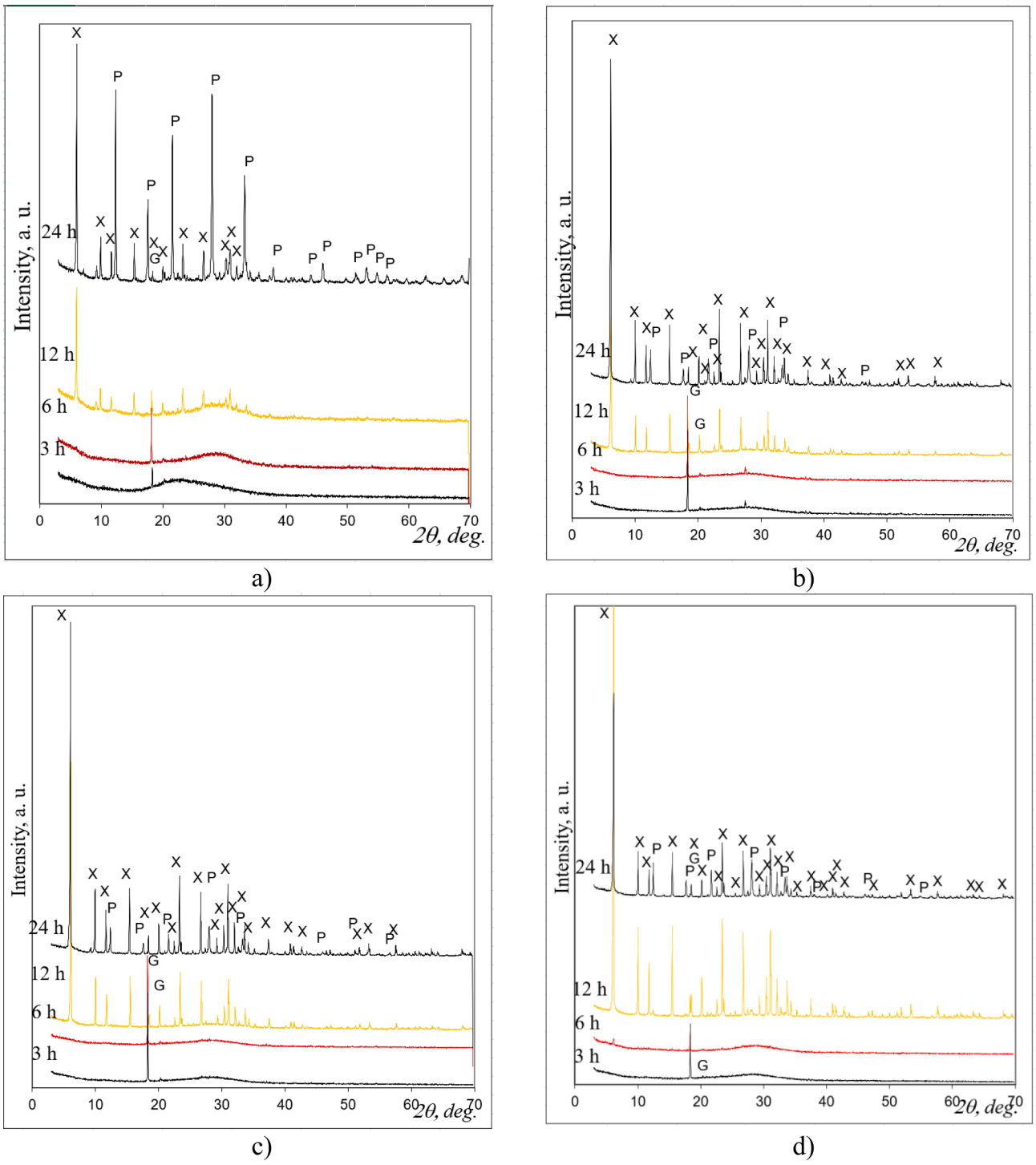

Fig. 3. The X-ray diffraction patterns of synthesis products. The durations of sonication: 0 min (a), 5 min (b) 10 min (c) and 20 min (d). The durations of hydrothermal treatment are 3 h, 6 h, 12 h and 24 h. Notes: X – Na-X, $Na_2Al_2Si_{2.5O9}{\cdot}6.2H_2O$, (38–237); P– $Na_6Al_6Si_{10}O_{32}(H_2O)_{12}$, (71–962) and G – gibbsite, $Al(OH)_3$, (43–577).

hydrothermal method (Fig. 3, a). It was observed that after 3 and 6 h any zeolites not formed. In these cases, the amorphous phase dominated in the synthesis products and it consisted 77% and 73% respectively after 3 (0S3H) and 6 h (0S6H) (Fig. 4). Only gibbsite as crystalline compound consisted the product of synthesis. After 12 h of synthesis (0S12H) the amount of amorphous phase decreased to 50% and Na-X zeolite (28%) and small amount (11%) of Na-P zeolite formed. About 8% of gibbsite left unreacted. In that cases when the duration of synthesis was 24 h Na-X zeolite zeolite converted to Na-P zeolite. In the synthesis products Na-P zeolite consisted about 54% and Na-X zeolite This conversion could be explained by the fact that the stability of Na-X zeolite was lower than that of Na-P zeolite [20]. Gibbsite was not detected, and it was completely transformed into zeolites.

The second series of zeolite synthesis were performed by combined hydrothermal treatment as most popular method of zeolite synthesis and sonication of initial aluminosilicates materials in alkaline media. The sonication duration of 5 min was chosen first (Fig. 3 b). It was indicated that after 3 and 6 h any zeolites formed. It was indicated that after 3 and

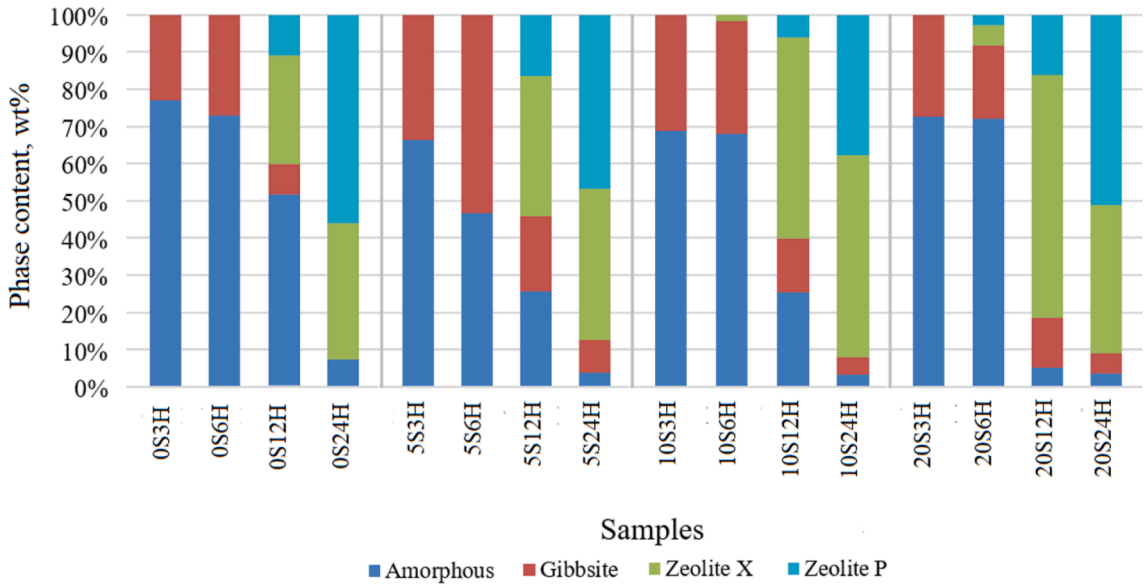

Fig. 4. The phase composition of synthesis products.

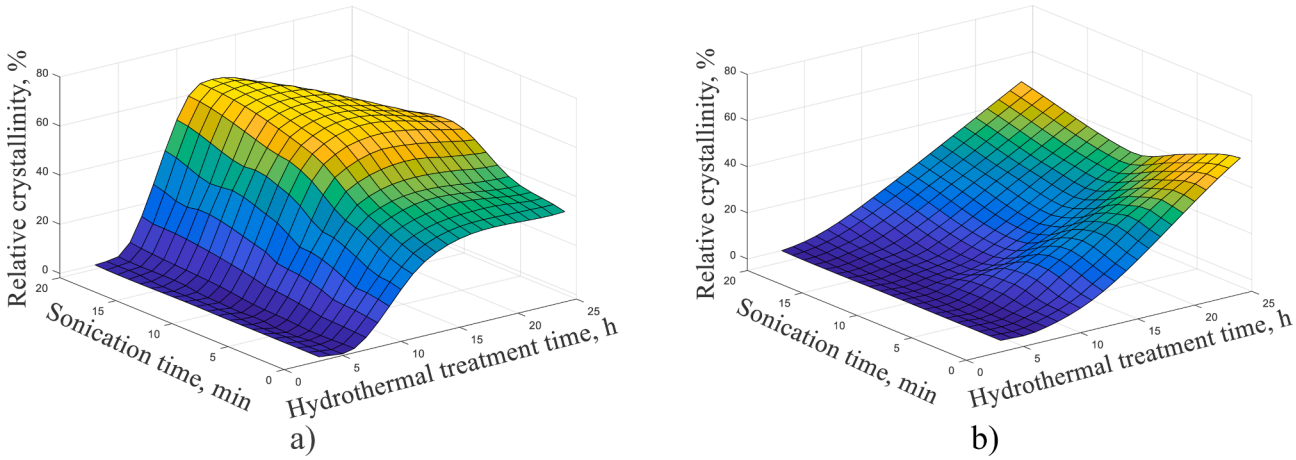

Fig. 5. Crystallization graphics of conversion of silica by-product to Na-X zeolite (a) and Na-P zeolite (b) using ultrasonic-assisted hydrothermal treatment.

6 h any zeolites were formed. The products of synthesis consisted only amorphous gel and gibbsite. The mixture of Na-X zeolite and Na-P zeolite formed when hydrothermal treatment was extended to 12 h and it consisted 38% and 16% respectively (Fig. 4). Finally, after 24 h of hydrothermal treatment some amount of Na-X zeolite convert to Na-P zeolite and in this case Na-P zeolite reached 46%.

Furthermore, the sonication time was prolonged to 10 min (Fig. 3 c). In this case when the hydrothermal curing was 3 h and 6 h amorphous phase and gibbsite dominated in the synthesis products. Only low intensity peaks of Na-X zeolite detected after 6 h of hydrothermal treatment and it consisted about 2%. After longer durations of hydrothermal treatment 12 h and 24 h significantly increased the intensity of peaks assigned to Na-X zeolite and Na-P zeolite. After 24 h of hydrothermal treatment Na-X zeolite consisted 53% and Na-P zeolite – 37% (Fig. 4).

When the sonication duration was 20 min any zeolites were not detected after 3 h of hydrothermal treatment (Fig. 3 d). When the treatment duration was lengthened into 6 h Na-X zeolite (6%) and Na-P zeolite (3%) began to form. Finally, after 12 h and 24 h of hydrothermal treatment Na-X zeolite and Na-P zeolite dominated in the synthesis product. After 24 h Na-X zeolite converts to Na-P zeolite. This could be explained with the higher stability of Na-P zeolite than Na-X zeolite. The 20S24H sample consisted 38% of Na-X zeolite and 48% of Na-P zeolite (Fig. 4).

During zeolite formation silica by-product participate in the reactions with NaOH as Al and Si source according to the Eq. (2) and (3).

$$2AlF_3{\cdot}3.5H_2O + 6NaOH \rightarrow 6NaF + 2Al(OH)_3 + 7H_2O \quad (2)$$

$$x\text{NaOH} + y\text{SiO}_2 + z\text{Al(OH)}_3 + n\text{H}_2\text{O} \rightarrow \text{Na-X zeolite and/or Na-P zeolite} \quad (3)$$

The progress of zeolitization reactions can be observed through changes in the mineral composition of the initial material and synthesis products which is shown in Fig. 5. In the product of synthesis, the maximal concentration of Na–X zeolite was getting after 20 min of sonication and 12 h of hydrothermal treatment (Fig. 5, a). Different situation with Na–P zeolite. In this case the highest crystallinity of this zeolite was without the sonication pretreatment (54%) and with 20 min of sonication accompanied by hydrothermal treatment (45%) of 24 h (Fig. 5, b). Moreover, the total amount of zeolites was in the range of 82–93% after 24 h of hydrothermal treatment followed or unfollowed by sonication (Table 2). Meanwhile, when hydrothermal treatment was shortened till 12 h the total amount of zeolites reached 82% (20S12H) and it was significantly higher than 0S12H (42%), 5S12H (55%) or 10S12H (61%).

According to Aldahri et al. [9], sonication increased the dissolution

Fig. 6. FTIR spectra of synthesis products: 0S24H, 20S12H and 20S12H.

of solid powders of initial materials in alkali solutions as a result of the mechanical effect. Initially cavitation helps to form crystallization centers and provides the energy needed for zeolite crystallization but in later stages of material decomposition destructive phenomena begin to prevail and the crystalline structure is partially destroyed. It has been observed from Fig. 5 that Na-X zeolite was converted into Na-P zeolite. This can be explained by the fact that the stability of Na-X zeolite was lower than that of Na-P zeolite. Using longer sonication and hydrothermal treatment times the nucleation of secondary zeolite phases such as Na-P zeolite formed as the result of the rearrangement and decomposition of the lattice of the primary crystals [21].

3.2. FTIR of zeolitic products

The vibrational spectra of zeolitic product were shown in Fig. 6. It was chosen three samples (0S24H, 20S12H and 20S24H) with the largest amount of Na-X and Na-P zeolites. In all curves stretch bands of isolated OH group in the spectral zone of around 3400 cm^{-1} was detected. These bands related with the interaction of OH group and the cations [23]. The bands occurring at 1651 cm^{-1} are attributed to H-OH flexion vibration. The strong bands at about 975 cm^{-1} are attributed to the asymmetric stretch vibration of Si–O or Al–O internal tetrahedral [23]. In the spectral region between 757 and 455 cm^{-1} the occurring bands could be attributed to both Na-X zeolite and Na-P zeolite.

The absorption bands at 749–757, 698, 609 and 455–466 cm^{-1} are typical of Na-P zeolite [27]. Na-X zeolite has main characteristic bands at 749–757, 680, 609 and 566 cm^{-1} and this is in agreement with the bands reported by Zhan et al. [23]. The symmetric stretches at 749–760 cm^{-1} were observed in both Na-X zeolite and Na-P zeolite. The next symmetric stretches at 680 cm^{-1} and 698 cm^{-1} are found in Na-P zeolite and Na-X zeolite samples. The bands at 566 cm^{-1} and 609 cm^{-1} are related with the double-ring vibration ant it is possible to detect only for Na-X zeolite [28]. In the synthesis products. The presence of Na-X type zeolite is indicated by a above mentioned bands at 566 cm^{-1} and 609 cm^{-1}. Na-P zeolite lack of double ring structural unite. The bending vibrations of tetrahedron Si(Al)-O at 455–466 cm^{-1} are found in both investigated zeolites [22,24].

The total amount of zeolites (about 90%) was similar for all investigated cases after 24 h of hydrothermal treatment (Fig. 4) and the intensity of bands almost the same. So, the results of FTIR spectroscopy analysis was encouraged the XRD analysis.

3.3. Microstructure of zeolitic products

The morphology of zeolitics samples is shown in the Fig. 5. Three types of samples with the highest amount of Na-P zeolite and Na-X zeolite were analyzed. By using only hydrothermal treatment without sonication after 24 h the mixture of Na-P zeolite and Na-X zeolite formed. In this sample dominated particles with pseudo-spherical forms (3 to 8 μm) constituted by small plates (Fig. 7, a, b). This shape of particles is typical of Na-P zeolite [25–27]. In addition to the particles of Na-P zeolite there are typical particles of Na-X zeolite. These particles had octahedron shape [28] with a size of 5 to 7 μm.

Different microstructure was detected when zeolites were synthesized by using ultrasonic-assisted hydrothermal treatment. After 12 h of hydrothermal treatment in 20S12H sample particles could be assigned to Na-X zeolite. In the synthesis product this zeolite consisted 64% and it had octahedron shape with a size of 3 to 6.5 μm (Fig. 7, b, c). In this case there are particles characteristic of Na-P zeolite. Two different types of morphologies were detected. One type is pseudo-spherical forms constituted by small plates (2 to 4 μm conglomerate) and second one had the morphology of “diamond” (3 to 6 μm). According to Huo et al [26] “diamond” shape particles are well crystallized Na-P zeolite with clear crystal edges. Moreover, small particles are attributed as amorphous phase.

After 20 min of sonication and 24 h of hydrothermal treatment only one type of morphologies of Na-P zeolite was detected. The amount of diamond shape particles assigned to Na-P zeolite has increased. The size of these particles was in range of 4 to 6 μm. The particles of Na-X zeolite were detected too with the shape of octahedron and the crystal size is about 0.5 to 1 μm. Besides Na-P zeolite and Na-X zeolite crystals small particles could be assigned as amorphous phase.

Therefore, sonication changed the morphology of Na-P zeolite and particles with pseudo-spherical forms constituted by small plates converted to “diamond” shape particles with clear crystal edges. Moreover, the sonication had influence on the formation smaller size zeolite crystals compared with the zeolite particles which forms by using only hydrothermal treatment [29].

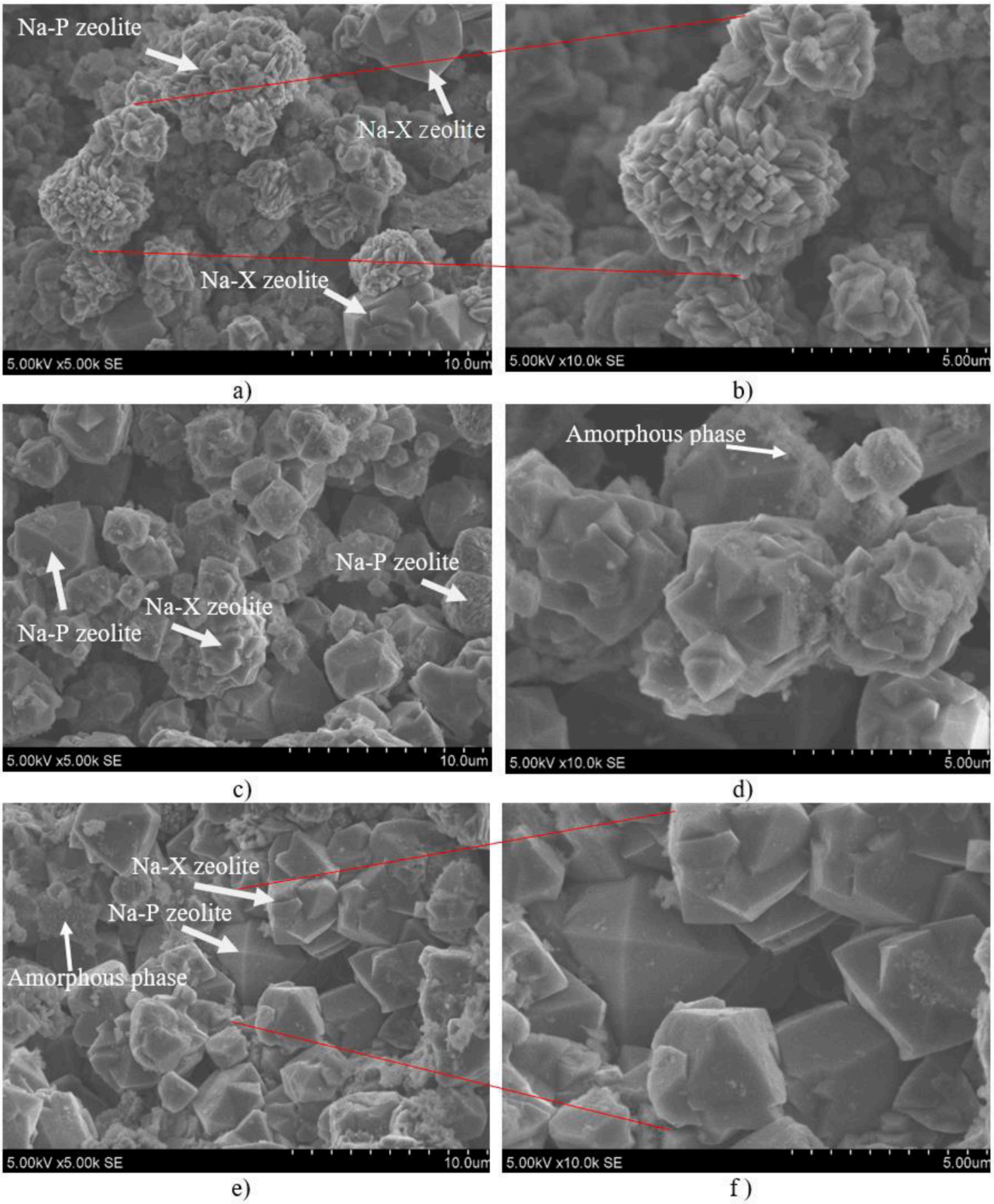

Fig. 7. Microstructure of synthesized products at different magnification (scale 5 μm and 10 μm). Notes: a, b – 0S24H; c, d – 20S12H e, f – 20S24H.

4. Conclusions

Silica by-product was transformed into zeolites by using sonochemical – hydrothermal treatment. These results show that utilization of silica by-product to zeolites is possible and this by-product can be a sustainable alternative to the traditional aluminosilicate initial materials.

The type, quantity of synthesized zeolites and its morphology is controlled by the time of sonication and hydrothermal treatment. During this treatment formed two types of zeolites: Na-P zeolite and Na-X zeolite. It was found that, sonication had positive influence on the conversion of the pseudo-spherical forms constituted by small plates of Na–P zeolite (primary crystallization form of Na-P zeolite) to clear crystal edges morphology (well crystallized Na-P zeolite). When the

sonication time was increased to 20 min the "diamond" morphology of Na–P zeolite dominated in the synthesis products. Without sonication pretreatment the pseudo-spherical forms constituted by small plates of Na–P zeolite formed. In all cases hydrothermal treatment was used. Furthermore, it was determined that ultrasonic-assisted hydrothermal treatment effected a reduction in the crystal size compared with the zeolites which were synthesized only by using hydrothermal treatment. Sonochemical pretreatment reduced the time of hydrothermal curing. It was shortened from 24 h (0S24H) to 12 h (10S12H or 20S12H) of hydrothermal treatment. The total amount of zeolites formed in the synthesis products was in the range of 88–93% for all investigated cases (without and with ultrasonic pretreatment) after 24 h of hydrothermal treatment. After shorter times (12 h) of hydrothermal treatment the total amount of zeolites increased twice from 42% (0S12H) till 82% (10S12H).

Declaration of Competing Interest

The authors declare that they have no known competing financial interests or personal relationships that could have appeared to influence the work reported in this paper.

References

[1] M. Yoldi, E.G. Fuentes-Ordoñez, S.A. Korili, A. Gil, Zeolite synthesis from industrial wastes, Microporous Mesoporous Mater. 287 (2019) 183–191, https://doi.org/10.1016/j.micromeso.2019.06.009.

[2] M. Osacký, H. Pálková, P. Hudec, A. Czímerová, D. Galusková, M. Vítková, Effect of alkaline synthesis conditions on mineralogy, chemistry and surface properties of phillipsite, P and X zeolitic materials prepared from fine powdered perlite by-product, Microporous Mesoporous Mater. 294 (2020) 109852, https://doi.org/10.1016/j.micromeso.2019.109852.

[3] T. Yang, C. Han, H. Liu, L. Yang, D. Liu, J. Tang, Y. Luo, Synthesis of Na-X zeolite from low aluminum coal fly ash: Characterization and high efficient As(V) removal, Adv. Powder Technol. 30 (1) (2019) 199–206, https://doi.org/10.1016/j.apt.2018.10.023.

[4] T. Fukasawa, A. Horigome, T. Tsu, A.D. Karisma, N. Maeda, A.-N. Huang, K. Fukui, Utilization of incineration fly ash from biomass power plants for zeolite synthesis from coal fly ash by hydrothermal treatment, Fuel Process. Technol. 167 (2017) 92–98, https://doi.org/10.1016/j.fuproc.2017.06.023.

[5] F.R.D. de Andrade, M.T.A.G. Yogi, E.B. Gomes, M.C. Shinzato, Extent of zeolite synthesis via alkaline fusion from tailings dam sediments, Environm. Earth Sc. 79 (2020) 1–9, https://doi.org/10.1007/s12665-020-09118-9.

[6] S.S. Bukhari, J. Behin, H. Kazemian, S. Rohani, Conversion of coal fly ash to zeolite utilizing microwave and ultrasound energies: A review, Fuel 140 (2015) 250–266, https://doi.org/10.1016/j.fuel.2014.09.077.

[7] Y. Liu, G. Wang, L.u. Wang, X. Li, Q. Luo, P. Na, Zeolite P synthesis based on fly ash and its removal of Cu(II) and Ni(II) ions, Chin. J. Chem. Eng. 27 (2) (2019) 341–348, https://doi.org/10.1016/j.cjche.2018.03.032.

[8] M.R. Abukhadra, S.M. Ibrahim, S.M. Yakout, M.E. El-Zaidy, A.A. Abdeltawab, Synthesis of Na+ trapped bentonite/zeolite-P composite as a novel catalyst for effective production of biodiesel from palm oil; Effect of ultrasonic irradiation and mechanism, Energy Convers. Manage. 196 (2019) 739–750, https://doi.org/10.1016/j.enconman.2019.06.027.

[9] T. Aldahri, J. Behin, H. Kazemian, S. Rohani, Synthesis of zeolite Na-P from coal fly ash by thermo-sonochemical treatment, Fuel 182 (2016) 494–501, https://doi.org/10.1016/j.fuel.2016.06.019.

[10] P. Pal, J.K. Das, N. Das, S. Bandyopadhyay, Synthesis of NaP zeolite at room temperature and short crystallization time by sonochemical method, Ultrason. Sonochem. 20 (1) (2013) 314–321, https://doi.org/10.1016/j.ultsonch.2012.07.012.

[11] M. Sayehi, G. Garbarino, G. Delahay, G. Busca, H. Tounsi, Synthesis of high value-added Na–P1 and Na-FAU zeolites using waste glass from fluorescent tubes and aluminum scraps, Mater. Chem. Phys. 248 (2020) 122903, https://doi.org/10.1016/j.matchemphys.2020.122903.

[12] D. Vaičiukynienė, A. Kantautas, V. Vaitkevičius, L. Jakevičius, Ž. Rudžionis, M. Paškevičius, Effects of ultrasonic treatment on zeolite NaA synthesized from by-product silica, Ultrason. Sonochem. 27 (2015) 515–521, https://doi.org/10.1016/j.ultsonch.2015.06.001.

[13] D. Vaičiukyniene V. Vaitkevičius A. Kantautas V. Sasnauskas Utilization of by-product waste silica in concrete - based materials Mat. Res. 15 4 561 567 10.1590/S1516-14392012005000082.

[14] V. Rudelis, T. Dambrauskas, A. Grinevičienė, K. Baltakys, The prospective approach for the reduction of fluoride ions mobility in industrial waste by creating products of commercial value, Sustainab. 11 (2019) 634, https://doi.org/10.3390/su11030634.

[15] D.S. Kim, J.-S. Chang, J.-S. Hwang, S.-E. Park, J.M. Kim, Synthesis of zeolite beta in fluoride media under microwave irradiation, Microporous Mesoporous Mater. 68 (1-3) (2004) 77–82, https://doi.org/10.1016/j.micromeso.2003.11.017.

[16] D. Jansen, C.h. Stabler, F. Goetz-Neunhoeffer, S. Dittrich, J. Neubauer, Does Ordinary Portland Cement contain amorphous phase? A quantitative study using an external standard method, Powder Diffr. 26 (1) (2011) 31–38, https://doi.org/10.1154/1.3549186.

[17] A. Larson, R. Dreele, General Structure Analysis System (GSAS). LAUR 86–748. https://11bm.xray.aps.anl.gov/documents/GSASManual.pdf, 2004 (accessed 31 July 2020).

[18] A. Iljina, K. Baltakys, M. Baltakys, R. Šiaučiūnas, Neutralization and removal of compounds containing fluoride ions from waste silica gel, Rev. Rom. Mater. 44 (2014) 265–271. http://solacolu.chim.upb.ro/p265-271web.pdf.

[19] R. Kaminskas, R. Kubiliute, Artificial pozzolana from silica gel waste–clay–limestone composite, Adv. Cem. Res. 26 (3) (2014) 155–168, https://doi.org/10.1680/adcr.13.00027.

[20] K. Bunmai, N. Osakoo, K. Deekamwong, C. Kosri, P. Khemthong, J. Wittayakun, Fast synthesis of zeolite NaP by crystallizing the NaY gel under microwave irradiation, Mater. Lett. 272 (2020) 127845, https://doi.org/10.1016/j.matlet.2020.127845.

[21] P. De Silva, K. Sagoe-Crenstil, Medium-term phase stability of Na_2O–Al_2O_3–SiO_2–H_2O geopolymer systems, Cem. Concr. Res. 38 (6) (2008) 870–876, https://doi.org/10.1016/j.cemconres.2007.10.003.

[22] X. Meng, X. Guo, Y. Zhong, Y. Pei, N. Chen, Q. Xie, Synthesis of a high-quality NaP zeolite from epidesmine by a hydrothermal method, Bull Mater Sci 42 (5) (2019), https://doi.org/10.1007/s12034-019-1918-x.

[23] B.-Z. Zhan, M.A. White, M. Lumsden, J. Mueller-Neuhaus, K.N. Robertson, T. S. Cameron, M. Gharghouri, Control of Particle Size and Surface Properties of Crystals of NaX Zeolite, Chem. Mater. 14 (9) (2002) 3636–3642, https://doi.org/10.1021/cm011635f.

[24] A.K. Kondru, P. Kumar, T.T. Teng, S. Chand, K.L. Wasewar, Synthesis and characterization of Na-Y zeolite from coal fly ash and its effectiveness in removal of dye from aqueous solution by wet peroxide oxidation, Archi. Environ. Sc. 5 (2011) 46–54.

[25] W. Ji, S. Zhang, P. Zhao, S. Zhang, N. Feng, L. Lan, Y. Ma, Green Synthesis Method and Application of NaP Zeolite Prepared by Coal Gasification Coarse Slag from Ningdong, Chin. Appl. Sc. 10 (2020) 2694, https://doi.org/10.3390/app10082694.

[26] Z. Huo, X. Xu, Z. Lü, J. Song, M. He, Z. Li, Q. Wang, L. Yan, Synthesis of zeolite NaP with controllable morphologies, Microporous Mesoporous Mater. 158 (2012) 137–140, https://doi.org/10.1016/j.micromeso.2012.03.026.

[27] D.F. Fitriyana, H. Suhaimi, R. Noferi, W. Caesarendra, Synthesis of Na-P Zeolite from Geothermal Sludge, in: R.I. Murakami, P.M. Koinkar, T. Fujii, T.G. Kim, H. Abdullah (Eds.), NAC 2019, Springer, Singapore, 2020, pp. 51-59. https://doi.org/10.1007/978-981-15-2294-9_5.

[28] J. Chen, X. Lu, Synthesis and characterization of zeolites NaA and NaX from coal gangue, J Mater Cycles Waste Manag 20 (1) (2018) 489–495, https://doi.org/10.1007/s10163-017-0605-5.

[29] X. Yin, Z. Long, C. Wang, Z. Li, M. Zhao, S. Yang, A time- and cost-effective synthesis of CHA zeolite with small size using ultrasonic-assisted method, Ultrason. Sonochem. 58 (2019) 104679, https://doi.org/10.1016/j.ultsonch.2019.104679.